Rapid Communications

Pressure effects on the electronic properties of the undoped superconductor ThFeAsN

N. Barbero,[1,*] S. Holenstein,[2,3] T. Shang,[2,4] Z. Shermadini,[2] F. Lochner,[5,6] I. Eremin,[6] C. Wang,[7] G.-H. Cao,[8,9] R. Khasanov,[2] H.-R. Ott,[1,2] J. Mesot,[1,2] and T. Shiroka[1,2]

[1]*Laboratorium für Festkörperphysik, ETH Zürich, CH-8093 Zurich, Switzerland*
[2]*Paul Scherrer Institut, CH-5232 Villigen PSI, Switzerland*
[3]*Physik-Institut der Universität Zürich, Winthertherstrasse 190, CH-8057, Zürich, Switzerland*
[4]*Institute of Condensed Matter Physics, EPFL Lausanne, CH-1015 Lausanne, Switzerland*
[5]*Max-Planck-Institut für Eisenforschung, D-40237 Düsseldorf, Germany*
[6]*Theoretische Physik III, Ruhr-Universität, D-44801 Bochum, Germany*
[7]*Department of Physics, Shandong University of Technology, Zibo 255049, China*
[8]*Department of Physics, State Key Laboratory of Silicon Materials, Zhejiang University, Hangzhou 310027, China*
[9]*Collaborative Innovation Center of Advanced Microstructures, Nanjing 210093, China*

(Received 31 January 2018; revised manuscript received 3 April 2018; published 13 April 2018)

The recently synthesized ThFeAsN iron pnictide superconductor exhibits a T_c of 30 K, the highest of the 1111-type series in the absence of chemical doping. To understand how pressure affects its electronic properties, we carried out microscopic investigations up to 3 GPa via magnetization, nuclear magnetic resonance, and muon-spin rotation experiments. The temperature dependence of the ^{75}As Knight shift, the spin-lattice relaxation rates, and the magnetic penetration depth suggest a multiband $s^{\pm}$-wave gap symmetry in the dirty limit, whereas the gap-to-T_c ratio Δ/k_BT_c hints at a strong-coupling scenario. Pressure modulates the geometrical parameters, thus reducing T_c as well as T_m, the temperature where magnetic-relaxation rates are maximized, both at the same rate of approximately -1.1 K/GPa. This decrease in T_c with pressure is consistent with band-structure calculations, which relate it to the deformation of the Fe $3d_{z^2}$ orbitals.

DOI: 10.1103/PhysRevB.97.140506

Introduction. The doping-induced superconductivity below $T_c = 26$ K in $LaFeAsO_{1-x}F_x$ [1] triggered long-term research interests towards iron-based superconductors (FeSCs), further boosted by the $T_c = 55$ K of $SmFeAsO_{1-\delta}$ [2]. Recently, we reported on superconducting properties of ThFeAsN [3], an undoped FeSC with a remarkable T_c of 30 K. Our data indicate that Fermi-surface modifications due to structural distortions and correlation effects may be as effective as doping in suppressing the antiferromagnetic order in favor of the formation of a superconducting phase. This is in contrast with most other REFeAsO-type compounds (RE = rare earth) where the quaternary parent compounds usually order magnetically and superconductivity is established via F [4–8] or H doping [9,10]. Due to strong electron correlations (compared with kinetic energy), iron pnictides are intermediately coupled systems. For this reason, the experimental values of T_c are distinctly higher than those calculated by assuming an electron-phonon coupling mechanism [11], which claims T_c values below 1 K. Among the strong-correlation effects, antiferromagnetic (AFM) spin fluctuations are widely accepted to mediate the SC pairing, but the detailed interaction model and an unequivocal identification of the gap symmetry are still being debated [12].

In an attempt to establish: (i) what causes the suppression of AFM order in nominally undoped FeSC compounds, (ii) why they become superconductors, and (iii) what determines their T_c values, we investigated ThFeAsN under applied hydrostatic pressure using different local probes. Hydrostatic and/or chemical pressure modify the structure and thus tune the T_c of iron-based superconductors, such as FeSe, whose original $T_c = 8.5$ K increases to 36.7 K at 8.9 GPa [13]. In particular, hydrostatic pressure is regarded as a *clean* tuning parameter for studying the effects of structural distortions on the electronic properties. A dependence of T_c on the crystallographic As-Fe-As bond angle [14] or on the anion height above the iron layers [15] h_{Pn} (see Fig. 1 in Mizuguchi *et al.* [15]) has previously been noted. With $a = 4.037$ and $c = 8.526$ Å [16], the tetragonal ($P4/nmm$) structure of ThFeAsN implies an $h_{Pn} = 1.305(4)$ Å, lower than the optimum anion height $h_{Pn}^{opt} = 1.38$ Å [15]. Hence, in the case of ThFeAsN, structural deformations induced by hydrostatic pressure would invariably lower T_c [16], in contrast to the above-mentioned FeSe case. To test this hypothesis and understand how pressure affects the electronic properties of an undoped 1111 superconducting compound, we performed magnetization, nuclear magnetic resonance (NMR), and muon-spin rotation (μSR) measurements on ThFeAsN under applied pressures up to 3 GPa.

First, we confirm experimentally the expected reduction of T_c with pressure. Then, on account of the T dependence of the NMR Knight shifts, spin-lattice relaxation rates, as well as μSR relaxation rates, we argue that the energy gap Δ of superconducting ThFeAsN adopts the $s^{\pm}$ symmetry, which persists up to at least 1.47 GPa. In the same pressure region, the ratio $R = \Delta/k_BT_c$ is reduced continuously from 2.16(3) at ambient pressure to 1.82(3) at 2.48(2) GPa, thus exceeding the BCS weak-coupling value of 1.76. The moderate

*nbarbero@phys.ethz.ch

variation of T_c with pressure is corroborated by results of band-structure calculations which imply only tiny changes in the electronic excitation spectrum around E_F. The abrupt quenching of magnetic excitations, as indicated by a cusp in $1/T_1T(T)$ at $T_m > T_c$, persists upon increasing pressure, and T_m is reduced at the same rate as T_c.

Synthesis and preliminary characterization. The polycrystalline ThFeAsN sample was synthesized via a high-temperature solid-state reaction as reported in Ref. [16]. X-ray diffraction and energy-dispersive x-ray measurements confirmed the absence of spurious phases (within ∼1%).

Magnetization measurements under applied pressure. The magnetization measurements were performed with a superconducting quantum interference device magnetic property management system-XL magnetometer. Preliminary measurements at ambient pressure revealed the presence of a tiny quantity of impurities (∼0.18%, assuming that they are of ferromagnetic nature) [3,16]. This, along with a broad drop-down in $M(T)$ data below T_c, related to defect-induced disorder, suggest that ThFeAsN in the SC phase should be described by models in the dirty limit. Hydrostatic pressures up to 3.1 GPa were achieved by means of a homemade diamond-anvil cell with a beryllium copper (BeCu) body. We chose Daphne Oil 7575 as the pressure-transmitting medium and a piece of lead to monitor the pressure [17]. For the magnetometry measurements we used a tiny piece of ThFeAsN ($m \sim 40\ \mu$g), whose magnetic response was on the order of 1.5–3 μemu. Because of the tiny signal, each measurement was performed with a background-subtraction procedure. Typical magnetization data at different applied pressures are shown in Fig. 1(a). The linearly decreasing trend of T_c, as determined from magnetization data, is shown in Fig. 2 (the red squares) and agrees well with the prediction of a reduced T_c at lower anion heights. A linear fit within the explored pressure range gives a slope of $\partial T_c/\partial p = -1.12 \pm 0.02$ K/GPa, similar to -1.5 K/GPa found in LiFeAs [19], another iron-based superconductor without doping.

NMR measurements under applied pressure. NMR measurements up to 1.47 GPa were performed using a BeCu piston-clamped high-pressure cell. The ^{75}As NMR investigations included line- and spin-lattice relaxation time (T_1) measurements in a magnetic field of 7.06 T [20]. T_1 values measured at both peaks of the central-transition line via inversion recovery resulted identical. Pressure was monitored *in situ* by using the nuclear quadrupolar resonance signal of ^{63}Cu in Cu_2O [21].

A typical ^{75}As NMR line at 7.06 T is shown in the inset of Fig. 1(c). Due to the large quadrupole moment of ^{75}As ($Q = 31.4$ fm^2), we considered only the central component of the NMR spectrum, which exhibits a typical second-order powder pattern with dipolar broadening. For temperatures from 4 to 295 K and hydrostatic pressures from zero up to 1.47 GPa, the central-line transition exhibits minor changes in shape and position. The spectra were fitted using the quadrupolar exact software (QUEST) [22], assuming no planar anisotropy ($\eta = 0$ as from experimental observations) and obtaining typical quadrupolar frequencies ν_Q of ∼5.6 MHz. The full width at half maximum (not shown) is negligibly affected by temperature or pressure, thus confirming the absence [3,23] of AFM long-range order, which would otherwise result in a remarkable broadening of the spectral lines starting at the onset of the transition.

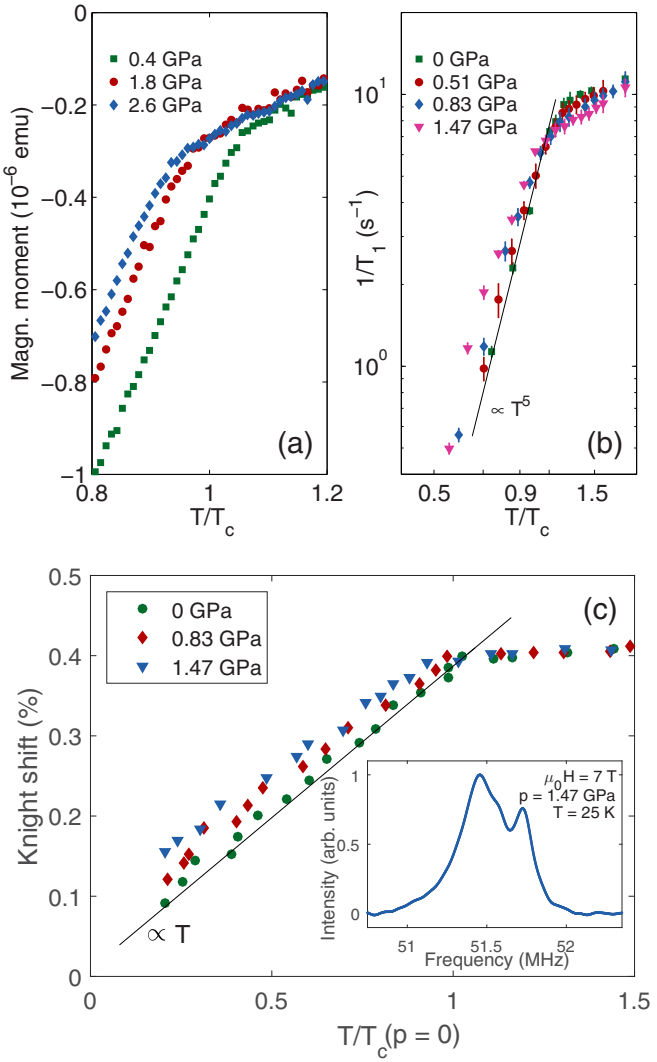

FIG. 1. (a) Temperature dependence of magnetization for selected applied pressures, measured at $\mu_0 H = 2$ mT. (b) ^{75}As NMR $1/T_1(T)$ data at ambient and at selected hydrostatic pressures. The line represents a T^5 behavior of relaxation with the exponent decreasing down to 3.6 at 1.47 GPa. To improve the readability of the plot, we do not indicate the T_m and T_c values, but we report them in Fig. 2. (c) Temperature dependence of the ^{75}As NMR Knight shift at three selected pressures. Uncertainties are on the order of the marker size. Inset: the ^{75}As NMR signal measured at 1.47 GPa, 7.06 T, and 25 K.

Figure 1(c) shows the Knight-shift $K_s(T) = (\nu - \nu_L)/\nu_L$ values as a function of temperature. At all the applied pressures, $K_s(T)$ exhibits a linearly decreasing trend below T_c, compatible with an $s^{\pm}$-wave scenario [12]. In fact, $K_s(T) \sim \mathrm{Re}\ \chi_S(q = 0, \omega \to 0)$, i.e., in the uniform susceptibility limit ($q = 0$), the interband scattering is suppressed, and the Knight-shift value includes only the independent contributions from the hole and electron bands [12,24]. In the clean limit, this implies an exponential temperature dependence for $K_s(T)$ in the $s^{\pm}$-wave case. However, as confirmed by magnetization data, our sample is not free of impurities. As reported in the literature [24–27], impurity self-energies form resonance states inside the SC gap

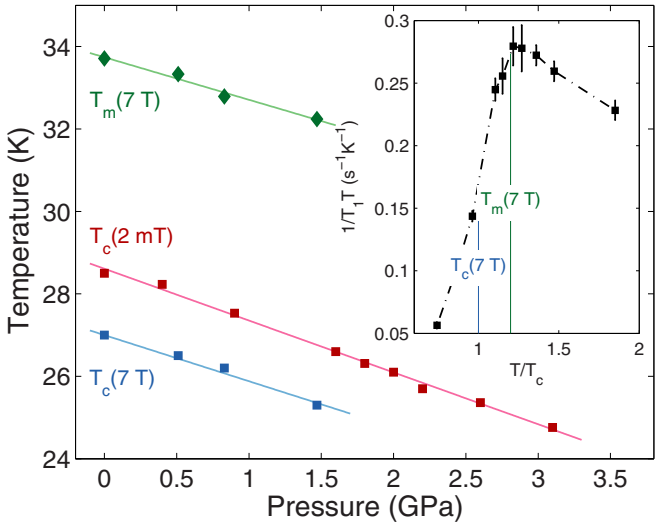

FIG. 2. Pressure dependence of T_m and T_c as determined via magnetometry and NMR measurements. T_m (the green diamonds) refers to the temperature where the electronic relaxation rates are maximized. Red and blue squares indicate the T_c values from magnetization measurements at 2 mT and from NMR measurements at 7 T, respectively. The inset shows the temperature dependence of $1/T_1T$ at ambient pressure, highlighting the maximum at T_m and a kink at T_c. Recently, a similar but broader feature in $1/T_1T$ of FeSe was attributed to a pseudogap behavior [18]. Note that, for ThFeAsN, $T_m \sim 1.2T_c$, at least up to 1.47 GPa.

and, thereby, affect the functional form of $K_s(T)$. The results of these calculations are compatible with the linear trend we observe. From the Knight-shift perspective, a dirty $s^{\pm}$-wave superconductor exhibits the features of a clean d-wave SC, but the latter interpretation is ruled out by the μSR data (see below). Quantitatively, the impurity effect is measured in terms of the $r \equiv \Gamma/\Delta$ ratio, where Γ is the impurity scattering rate and Δ is the SC gap value. The critical value separating the exponential from the linear behavior is $r_{\rm cr} = 0.045$ [12,24]. Although we cannot provide an estimate for the r value, the observed linear dependence of $K_s(T)$ suggests that, in our case, $r > r_{\rm cr}$.

From the peak separation of the second-order quadrupole-broadened powder spectra of the central transition [see Fig. 1(c) inset] $\Delta f = f_{\rm right} - f_{\rm left}$, one can evaluate the electric-field gradient component $eq = V_{zz} = 2I(2I-1)h\nu_Q/(3eQ)$. Here ν_Q is obtained from the quadrupole splitting frequency via

$$\Delta f = \frac{\frac{25}{9}\left[I(I+1) - \frac{3}{4}\right]\nu_Q^2}{16\nu_L}. \qquad (1)$$

We observe that pressure reduces the distance between the peaks. This implies a slight *symmetry enhancement* upon increasing pressure, resulting in $eq \equiv V_{zz}$ values of -1.65×10^{21} and -1.45×10^{21} V/m^2 at ambient pressure and 1.47 GPa, respectively.

To study the electron-spin dynamics, the temperature dependence of the nuclear spin-lattice relaxation rate $1/T_1$ was measured at different pressures as shown in Fig. 1(b). At all pressures, $1/T_1(T)$ exhibits a kink, resulting in a maximum at T_m if plotted as $1/(T_1T)$ (see the inset of Fig. 2). The data above T_m reveal an additional relaxation channel due to short-range AFM spin fluctuations as shown by Mössbauer [23] and ambient-pressure NMR [3] results, the latter extending to values of $T/T_m < 0.5$. Below T_m this relaxation channel is increasingly inhibited before the onset of superconductivity at T_c, which reduces $1/(T_1T)$ even further. Note that, as shown in Fig. 2, $T_m(p)$ decreases monotonously by -1.0 ± 0.1 K/GPa, i.e., virtually with the same slope as $\partial T_c/\partial p$. The T_c values (the onset of SC transition) were determined from 2-mT magnetization measurements (the red squares) and from the maxima of the T derivative of the NMR spin-lattice relaxation data at 7.06 T (the blue squares) as described in the Supplemental Material [28].

In several 1111 FeSCs, the T^3 dependence [29,30] of $1/T_1(T)$ suggests a nodal gap, however, ruled out by angle-resolved photoemission spectroscopy experiments [31]. By employing $\mathcal{T}$-matrix theory, the impurity-scattering effect has been included in the modeling of the $1/T_1(T)$ dependence [32]. For $r = 0$, one obtains the exponential behavior of $1/T_1(T)$ expected for an $s^{\pm}$ wave [33], whereas for $r = r_{\rm cr}$ one finds $1/T_1(T) \propto T^3$ and a suppression of the Hebel-Slichter coherence peak [34], in good agreement with experiments [29]. Our data, shown in Fig. 1(b), exhibit an even steeper T dependence of the type $1/T_1(T) \propto T^5$ as previously reported for other FeSCs [27,35]. Such a T^5 behavior does not require a different gap symmetry if strong-coupling effects are taken into account as discussed in the Introduction. According to theoretical estimates, a $R \equiv \Delta/k_BT_c = 2.5$ ratio in a dirty-limit sample with $r = r_{\rm cr}$ gives rise to the observed T^5 power-law behavior [34]. The reduction of the power-law exponent from 5 to 3.6 for pressures from zero to 1.47 GPa indicates a pressure-induced weakening of the coupling, in good agreement with our μSR results (see below). The same results also rule out a clean d-wave superconductivity scenario and are compatible with an iso-/anisotropic s- or $s^{\pm}$-wave model for ThFeAsN [3,36].

Transverse-field-μSR measurements under high pressure. The μSR investigations were performed at the general purpose (GPS) (ambient pressure) and the general purpose decay-channel (GPD) (high-pressure) spectrometers of the Paul Scherrer Institut, Villigen. Since the high-pressure measurements require a relatively large sample mass (~2 g), a new polycrystalline sample with $T_c = 27$ K was prepared. The lower T_c is due to a different preparation protocol. The GPS measurements on the new batch confirmed the earlier findings [3] and were used as a reference to analyze the high-pressure data. The muon fraction stopping in the pressure cell ($f_{\rm cell} = 60\%$) was determined by fitting a zero-field (ZF) spectrum with the cell relaxation rates fixed at their literature values [37] and the sample relaxation rate fixed at the GPS value, hence leaving the muon stopping fraction as the only free parameter. The absence of significant changes with temperature in the ZF relaxation rate of the sample, even at the highest pressure, rules out a possible pressure-induced magnetic order. Thus, we focused on the TF measurements in the SC region, carried out at 70 mT. The data were analyzed using

$$A(t)/A_0 = (1 - f_{\rm cell})\cos(\gamma_\mu B_{\rm sc}t + \phi)\exp\left(-\lambda_{\rm sc}t - \sigma_{\rm sc}^2t^2/2\right) + f_{\rm cell}\cos(\gamma_\mu B_{\rm cell}t + \phi)\exp\left(-\lambda_{\rm cell}t - \sigma_{\rm cell}^2t^2/2\right),$$

where A_0 is the initial asymmetry, γ_μ is the muon gyromagnetic ratio, B is the local field at the muon stopping site, ϕ is the

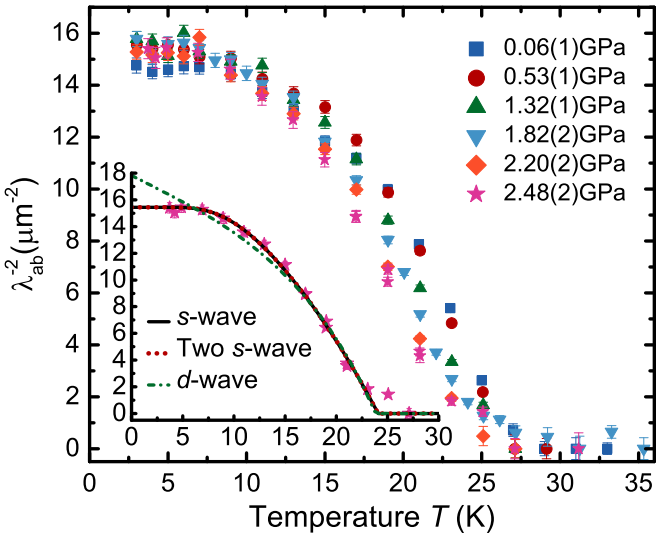

FIG. 3. Temperature dependence of λ_{ab}^{-2} as extracted from TF-μSR measurements shows a suppression of T_c with pressure but no changes in functional form. The inset: Fits of $\lambda_{ab}^{-2}(T)$ data taken at the highest pressure by using different SC models. Note that the one-gap and the two-gap s-wave models overlap perfectly.

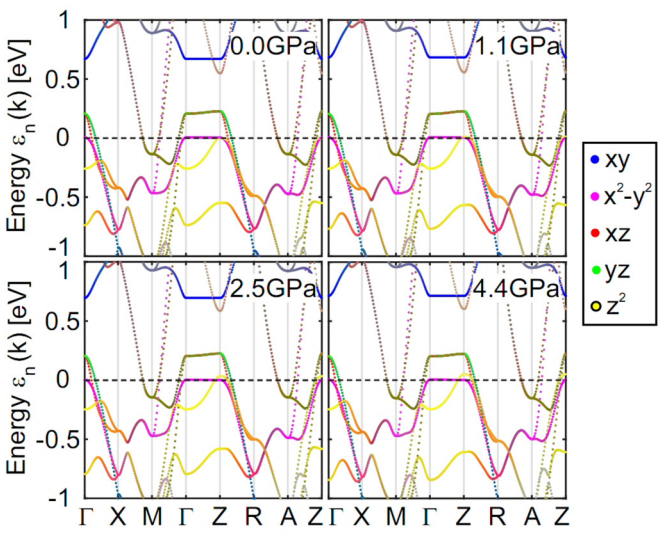

FIG. 4. ThFeAsN band-structure calculations upon increasing pressure. Note the lack of major changes at the Fermi-energy level except for a minor change in the $3d_{z^2}$ orbitals close to the Z point.

initial phase, and λ and σ are the exponential and Gaussian relaxation rates, whose subscript labels denote the parameters for muons stopping in the sample and the cell, respectively. To ensure a robust fit, the changes in $B_{\rm cell}$ and $\sigma_{\rm cell}$ were related to the field shift in the sample relative to $B_{\rm ext}$ [38],

$$B_{\rm cell}(T) = B_{\rm ext} + c_1[B_{\rm ext} - B_{\rm sc}(T)],$$
$$\sigma_{\rm cell}^2(T) = \sigma_{\rm cell}^2(T > T_c) + c_2^2(B_{\rm ext} - B_{\rm sc})^2. \quad (2)$$

where c_1 and c_2 are proportionality constants. Since $\lambda_{\rm cell}$ varies with temperature, its intrinsic T dependence was determined by requiring that the zero-pressure GPD measurements reproduce the GPS results from which we evaluated an average penetration depth of $\lambda_{ab}(0\ {\rm K}) = 255(1)$ nm. As can be seen from the temperature dependence of the inverse-squared penetration depth [39], hydrostatic pressure reduces the superconducting T_c [at a rate of 1.1(2) K/GPa] while barely influencing the gap symmetry. The latter is clearly not of a clean d-wave type as shown by the poor fit of the highest-pressure dataset (see the inset of Fig. 3), whereas a dirty d-wave scenario is already excluded by the NMR measurements. Our data fit, with the same accuracy, a single- or a two-gap s-wave model (the latter yields two gaps of almost equal magnitude). Hence, μSR data are compatible with an s-wave model, but there is no strong evidence for claiming ThFeAsN to be a double-gap superconductor. Interestingly, the gap value is suppressed faster [from 5.0(1) meV at 0.06(1) GPa to 3.8(1) meV at 2.48(2) GPa] than T_c, hence implying a reduction of the $\Delta(0)/k_{\rm B}T_c$ ratio from 2.16(3) to 1.82(3) upon increasing pressure, the latter being closer to the BCS value of 1.76. The absence of a magnetic order even at the highest pressures suggests that the reduction of T_c is of structural origin. The lack of AFM order as confirmed by both NMR and zero-field μSR data has no clear explanation [3]. An educated guess [40] suggests intrinsic disorder as the key reason to prevent AFM order.

Band-structure calculations. For the density functional theory (DFT) calculations we resorted to the Vienna *ab initio* simulation package (VASP) [41–43] with the projector augmented wave [44] basis and made use of the measured ThFeAsN crystal parameters [16]. Hereby, we use VASP in the generalized-gradient approximation [45] and show in Fig. 4 the resulting band-structure evolution with pressure. One can rule out substantial pressure effects on the electronic structure—within the accuracy of band-structure calculations—including here changes in the effective mass. For the experimentally accessible pressure values, we find insignificant modifications of the electronic structure except for a minor change in the $3d_{z^2}$ orbitals close to the Z point.

This lack of substantial pressure effects raises the question of the origin of T_c suppression in this compound. We recall that the electronic properties of ThFeAsN are similar to those of $LaFeAsO_{0.9}F_{0.1}$ and that, as shown above, ThFeAsN can be regarded as a superconductor in the dirty limit [40]. In this case, despite a nested electronic structure, the AFM ordering of excitonic type is more sensitive to disorder than is the $s^{\pm}$-wave superconductivity [46–49]. Hence, in the nominally undoped compound, disorder tends to promote the $s^{\pm}$ states over the AFM ordering. Indeed, disorder affects the magnetic order by lowering $T_{\rm N}$, whereas, in the case of superconductivity, the inter-/intraband scattering plays a major role, and only the interband impurity scattering lowers the T_c. This may explain why, in contrast to the cleaner LaFeAsO, ThFeAsN is a superconductor instead of an antiferromagnet, although both are nominally undoped compounds.

As reported in Ref. [50], in doped LaFeAsO hydrostatic pressure does not influence T_c, although the superfluid density is enhanced. In fact, pressure seems to slightly change the ratio of intra- to interband impurity scattering without sensibly affecting T_c. The most plausible reason for the lowering of T_c with pressure in ThFeAsN could be a subtle modification of the electronic structure (beyond density functional theory), which can account for the simultaneous suppression of the

AFM fluctuations and of the SC. For example, smaller Fermi-surface pockets (with respect to simulations) would imply a much stronger effect of pressure on the electronic structure. Nearly all iron-based superconductors, including the LaFeAsO family, exhibit an unusual renormalization of the electronic structure, which results in much smaller Fermi-surface pockets than anticipated from DFT calculations [51]. By assuming such a renormalization, i.e., the so-called red/blueshift for the pockets, one may justify the suppression of AFM fluctuations and SC in ThFeAsN as well.

Conclusion. In ThFeAsN, the Knight-shift $K(T)$, the spin-lattice relaxation times $T_1(T)$, and the London penetration depth $\lambda(T)$ indicate that pressure reduces T_c [$\partial T_c/\partial p = -1.12(2)$ K/GPa] and weakens the pairing interaction as measured by the ratio $\Delta/k_B T_c$. Interestingly, $T_m(p)$ too is reduced by pressure at the same rate of T_c, confirming that magnetic excitations which reflect AFM spin fluctuations, whereas competing with superconductivity, play an essential role in the pairing process. Finally, our experimental data and DFT calculations indicate an $s^{\pm}$ SC order parameter independent of pressure and suggest that intrinsic disorder plays a key role in suppressing antiferromagnetism in ThFeAsN.

Acknowledgments. The authors thank H. Luetkens for useful discussions. This Rapid Communication was financially supported, in part, by the Schweizerische Nationalfonds zur Förderung der Wissenschaftlichen Forschung (SNF), through the SNF Funds No. 200021-159736 and 200021-169455.

[1] Y. Kamihara, T. Watanabe, M. Hirano, and H. Hosono, Iron-based layered superconductor La[$O_{1-x}F_x$]FeAs ($x = 0.05$–0.12) with $T_c = 26$ K, J. Am. Chem. Soc. **130**, 3296 (2008).

[2] Z.-A. Ren, G.-C. Che, X.-L. Dong, J. Yang, W. Lu, W. Yi, X.-L. Shen, Z.-C. Li, L.-L. Sun, F. Zhou, and Z.-X. Zhao, Superconductivity and phase diagram in iron-based arsenic-oxides $ReFeAsO_{1-\delta}$ (Re = rare-earth metal) without fluorine doping, Eurphys. Lett. **83**, 17002 (2008).

[3] T. Shiroka, T. Shang, C. Wang, G.-H. Cao, I. Eremin, H.-R. Ott, and J. Mesot, High-T_c superconductivity in undoped ThFeAsN, Nat. Commun. **8**, 156 (2017).

[4] H.-H. Wen, Developments and perspectives of iron-based high-temperature superconductors, Adv. Mater. **20**, 3764 (2008).

[5] M. V. Sadovskii, High-temperature superconductivity in iron-based layered iron compounds, Phys.-Usp. **51**, 1201 (2008).

[6] J. Paglione and R. L. Greene, High-temperature superconductivity in iron-based materials, Nat. Phys. **6**, 645 (2010).

[7] D. C. Johnston, The puzzle of high temperature superconductivity in layered iron pnictides and chalcogenides, Adv. Phys. **59**, 803 (2010).

[8] Q. Si, R. Yu, and E. Abrahams, High-temperature superconductivity in iron pnictides and chalcogenides, Nat. Rev. Mater. **1**, 16017 (2016).

[9] Y. Muraba, S. Matsuishi, and H. Hosono, La-substituted CaFeAsH superconductor with $T_c = 47$ K, J. Phys. Soc. Jpn. **83**, 033705 (2014).

[10] Y. Muraba, S. Iimura, S. Matsuishi, and H. Hosono, Hydrogen-substituted superconductors $SmFeAsO_{1-x}H_x$ misidentified as oxygen-deficient $SmFeAsO_{1-x}$, Inorg. Chem. **54**, 11567 (2015).

[11] L. Boeri, O. V. Dolgov, and A. A. Golubov, Is $LaFeAsO_{1-x}F_x$ an Electron-Phonon Superconductor? Phys. Rev. Lett. **101**, 026403 (2008).

[12] Y. Bang and G. R. Stewart, Superconducting properties of the $s^{\pm}$-wave state: Fe-based superconductors, J. Phys.: Condens. Matter **29**, 123003 (2017).

[13] T. M. McQueen, I. A. Troyan, T. Palasyuk, M. I. Eremets, R. J. Cava, S. Naghavi, F. Casper, V. Ksenofontov, G. Wortmann, and C. Felser, Electronic and magnetic phase diagram of β-$Fe_{1.01}$ Se with superconductivity at 36.7 K under pressure, Nat. Mater. **8**, 630 (2009).

[14] C.-H. Lee, H. Eisaki, H. Kito, M. T. Fernandez-Diaz, T. Ito, K. Kihou, H. Matsushita, M. Braden, and K. Yamada, Effect of structural parameters on superconductivity in fluorine-free $LnFeAsO_{1-y}$ (Ln = La, Nd), J. Phys. Soc. Jpn. **77**, 083704 (2008).

[15] Y. Mizuguchi, Y. Hara, K. Deguchi, S. Tsuda, T. Yamaguchi, K. Takeda, H. Kotegawa, H. Tou, and Y. Takano, Anion height dependence of T_c for the Fe-based superconductor, Supercond. Sci. Technol. **23**, 054013 (2010).

[16] C. Wang, Z.-C. Wang, Y.-X. Mei, Y.-K. Li, L. Li, Z.-T. Tang, Y. Liu, P. Zhang, H.-F. Zhai, Z.-A. Xu, and G.-H. Cao, A new ZrCuSiAs-type superconductor: ThFeAsN, J. Am. Chem. Soc. **138**, 2170 (2016).

[17] A. Eiling and J. S. Schilling, Pressure and temperature dependence of electrical resistivity of Pb and Sn from 1–300 K and 0–10 GPa–use as continuous resistive pressure monitor accurate over wide temperature range; superconductivity under pressure in Pb, Sn and In, J. Phys. F **11**, 623 (1981).

[18] A. Shi, T. Arai, S. Kitagawa, T. Yamanaka, K. Ishida, A. E. Böhmer, C. Meingast, T. Wolf, M. Hirata, and T. Sasaki, Pseudogap behavior of the nuclear spin-lattice relaxation rate in FeSe probed by ^{77}Se-NMR, J. Phys. Soc. Jpn. **87**, 013704 (2018).

[19] M. Gooch, B. Lv, J. H. Tapp, Z. Tang, B. Lorenz, A. M. Guloy, and P. C. W. Chu, Pressure shift of the superconducting T_c of LiFeAs, Europhys. Lett. **85**, 27005 (2009).

[20] ^{75}As with spin $I = 3/2$ and Larmor frequency $\nu_L = 51.523$ MHz at 7.06 T was chosen because it occupies a single site and is sensitive to the structural and electronic variations in the FeAs layers under pressure. The ^{75}As NMR spectra were obtained via fast Fourier transformation of spin-echo signals generated by $\pi/2$-π rf pulses of 2 and 4 μs, respectively, with recycle delays ranging from 0.1 s at room temperature up to 6 s at 5 K and echo times of 50 μs. Given the long rf-pulse length, frequency sweeps in 40-kHz steps were used to cover the spectrum central transition (∼1-MHz wide).

[21] A. P. Reyes, E. T. Ahrens, R. H. Heffner, P. C. Hammel, and J. D. Thompson, Cuprous oxide manometer for high pressure magnetic resonance experiments, Rev. Sci. Instrum. **63**, 3120 (1992).

[22] F. A. Perras, M. W. Cory, and D. L. Bryce, QUEST – QUadrupolar Exact SofTware: A fast graphical program for the exact simulation of NMR and NQR spectra for quadrupolar nuclei, Solid State Nucl. Magn. Reson. **45-46**, 36 (2012).

[23] M. A. Albedah, F. Nejadsattari, Z. M. Stadnik, Z.-C. Wang, C. Wang, and G.-H. Cao, Absence of the stripe antiferromagnetic order in the new 30 K superconductor ThFeAsN, J. Alloys Compd. **695**, 1128 (2017).

[24] Y. Bang and H.-Y. Choi, Possible pairing states of the Fe-based superconductors, Phys. Rev. B **78**, 134523 (2008).

[25] A. Kawabata, S. C. Lee, T. Moyoshi, Y. Kobayashi, and M. Sato, Superconductivity of $LaFe_{1-y}Co_yAsO_{1-x}F_x$, J. Phys. Soc. Jpn. **77**, 103704 (2008).

[26] K. Matano, Z. A. Ren, X. L. Dong, L. L. Sun, Z. X. Zhao, and G. Zheng, Spin-singlet superconductivity with multiple gaps in $PrFeAsO_{0.89}F_{0.11}$, Europhys. Lett. **83**, 57001 (2008).

[27] Y. Nakai, T. Iye, S. Kitagawa, K. Ishida, S. Kasahara, T. Shibauchi, Y. Matsuda, and T. Terashima, ^{31}P and ^{75}As NMR evidence for a residual density of states at zero energy in superconducting $BaFe_2(As_{0.67}P_{0.33})_2$, Phys. Rev. B **81**, 020503 (2010).

[28] See Supplemental Material at http://link.aps.org/supplemental/10.1103/PhysRevB.97.140506 for the plot of the T derivative of the $1/T_1T(T)$ curve and the definitions of T_m and T_c.

[29] S. Kawasaki, K. Shimada, G. F. Chen, J. L. Luo, N. L. Wang, and G. Q. Zheng, Two superconducting gaps in $LaOFeAsO_{0.92}F_{0.08}$ revealed by ^{75}As nuclear quadrupole resonance, Phys. Rev. B **78**, 220506 (2008).

[30] H. Mukuda, N. Terasaki, N. Tamura, H. Kinouchi, M. Yashima, Y. Kitaoka, K. Miyazawa, P. M. Shirage, S. Suzuki, S. Miyasaka, S. Tajima, H. Kito, H. Eisaki, and A. Iyo, Doping dependence of normal-state properties in iron-based oxypnictide superconductor $LaFeAsO_{1-y}$ probed by ^{57}Fe-NMR and ^{75}As-NMR/NQR, J. Phys. Soc. Jpn. **78**, 084717 (2009).

[31] H. Ding, P. Richard, K. Nakayama, K. Sugawara, T. Arakane, Y. Sekiba, A. Takayama, S. Souma, T. Sato, T. Takahashi, Z. Wang, X. Dai, Z. Fang, G. F. Chen, J. L. Luo, and N. L. Wang, Observation of Fermi-surface-dependent nodeless superconducting gaps in $Ba_{0.6}K_{0.4}Fe_2As_2$, Europhys. Lett. **83**, 47001 (2008).

[32] W. Ziegler, D. Poilblanc, R. Preuss, W. Hanke, and D. J. Scalapino, *T*-matrix formulation of impurity scattering in correlated systems, Phys. Rev. B **53**, 8704 (1996).

[33] T. Oka, Z. Li, S. Kawasaki, G. F. Chen, N. L. Wang, and G. Q. Zheng, Antiferromagnetic Spin Fluctuations Above the Dome-Shaped and Full-Gap Superconducting States of $LaFeAsO_{1-x}F_x$ Revealed by ^{75}As-Nuclear Quadrupole Resonance, Phys. Rev. Lett. **108**, 047001 (2012).

[34] Y. Bang, H.-Y. Choi, and H. Won, Impurity effects on the $s^{\pm}$-wave state of the iron-based superconductors, Phys. Rev. B **79**, 054529 (2009).

[35] K. Matano, Z. Li, G. L. Sun, D. L. Sun, C. T. Lin, M. Ichioka, and G. Zheng, Anisotropic spin fluctuations and multiple superconducting gaps in hole-doped $Ba_{0.72}K_{0.28}Fe_2As_2$: NMR in a single crystal, Europhys. Lett. **87**, 27012 (2009).

[36] D. Adroja, A. Bhattacharyya, P. K. Biswas, M. Smidman, A. D. Hillier, H. Mao, H. Luo, G.-H. Cao, Z. Wang, and C. Wang, Multigap superconductivity in ThAsFeN investigated using μSR measurements, Phys. Rev. B **96**, 144502 (2017).

[37] R. Khasanov, Z. Guguchia, A. Maisuradze, D. Andreica, M. Elender, A. Raselli, Z. Shermadini, T. Goko, F. Knecht, E. Morenzoni, and A. Amato, High pressure research using muons at the Paul Scherrer Institute, High Pressure Res. **36**, 140 (2016).

[38] A. Maisuradze, A. Shengelaya, A. Amato, E. Pomjakushina, and H. Keller, Muon spin rotation investigation of the pressure effect on the magnetic penetration depth in $YBa_2Cu_3O_x$, Phys. Rev. B **84**, 184523 (2011).

[39] The penetration depth was calculated from $\sigma_{sc}(T)$ and is proportional to the superfluid density .

[40] We recall that the transport and magnetic properties of ThFeAsN are similar to those of $LaFeAsO_{0.9}F_{0.1}$ [3], which indicates that the absence of a long-range magnetic order in the nominally undoped ThFeAsN can be due to intrinsic disorder. It is known that the long-range antiferromagnetic order in the iron-based superconductors can be even destroyed by nonmagnetic impurities, despite the electron-band structure remaining unchanged with respect to the undoped case [46,47]. The resulting phase diagram is similar to that obtained by introducing extra holes or electrons in the FeAs layers. Theoretically, this can be understood as a result of the stronger effect of nonmagnetic impurities on the AFM order than on the multiband $s^{\pm}$-wave superconductivity [48]. Although both the intra- and the interband impurity scatterings are destructive for the long-range AFM order, only the interband scattering is pair breaking for an $s^{\pm}$ superconducting state.

[41] G. Kresse and J. Hafner, *Ab initio* molecular dynamics for liquid metals, Phys. Rev. B **47**, 558(R) (1993).

[42] G. Kresse and J. Furthmüller, Efficiency of *ab-initio* total energy calculations for metals and semiconductors using a plane-wave basis set, Comput. Mater. Sci. **6**, 15 (1996).

[43] G. Kresse and J. Furthmüller, Efficient iterative schemes for *ab initio* total-energy calculations using a plane-wave basis set, Phys. Rev. B **54**, 11169 (1996).

[44] P. E. Blöchl, Projector augmented-wave method, Phys. Rev. B **50**, 17953 (1994).

[45] J. P. Perdew, K. Burke, and M. Ernzerhof, Generalized Gradient Approximation Made Simple, Phys. Rev. Lett. **77**, 3865 (1996).

[46] V. Brouet, F. Rullier-Albenque, M. Marsi, B. Mansart, M. Aichhorn, S. Biermann, J. Faure, L. Perfetti, A. Taleb-Ibrahimi, P. Le Fèvre, F. Bertran, A. Forget, and D. Colson, Significant Reduction of Electronic Correlations Upon Isovalent Ru Substitution of $BaFe_2As_2$, Phys. Rev. Lett. **105**, 087001 (2010).

[47] R. S. Dhaka, C. Liu, R. M. Fernandes, R. Jiang, C. P. Strehlow, T. Kondo, A. Thaler, J. Schmalian, S. L. Bud'ko, P. C. Canfield, and A. Kaminski, What Controls the Phase Diagram and Superconductivity in Ru-substituted $BaFe_2As_2$? Phys. Rev. Lett. **107**, 267002 (2011).

[48] M. G. Vavilov and A. V. Chubukov, Phase diagram of iron pnictides if doping acts as a source of disorder, Phys. Rev. B **84**, 214521 (2011).

[49] G. Lang, L. Veyrat, U. Gräfe, F. Hammerath, D. Paar, G. Behr, S. Wurmehl, and H.-J. Grafe, Spatial competition of the ground states in 1111 iron pnictides, Phys. Rev. B **94**, 014514 (2016).

[50] G. Prando, T. Hartmann, W. Schottenhamel, Z. Guguchia, S. Sanna, F. Ahn, I. Nekrasov, C. G. F. Blum, A. U. B. Wolter, S. Wurmehl, R. Khasanov, I. Eremin, and B. Büchner, Mutual Independence of Critical Temperature and Superfluid Density Under Pressure in Optimally Electron-Doped Superconducting $LaOFeAsO_{1-x}F_x$, Phys. Rev. Lett. **114**, 247004 (2015).

[51] A. Charnukha, D. V. Evtushinsky, C. E. Matt, N. Xu, M. Shi, B. Büchner, N. D. Zhigadlo, B. Batlogg, and S. V. Borisenko, High-temperature superconductivity from fine-tuning of Fermi-surface singularities in iron oxypnictides, Sci. Rep. **5**, 18273 (2015).